Sign problem in Monte Carlo simulations of frustrated quantum spin systems

Patrik Henelius*
National High Magnetic Field Laboratory, 1800 East Paul Dirac Drive, Tallahassee, Florida 32310

Anders W. Sandvik
Department of Physics, University of Illinois at Urbana-Champaign, 1110 West Green Street, Urbana, Illinois 61801
(Received 24 January 2000)

We discuss the sign problem arising in Monte Carlo simulations of frustrated quantum spin systems. We show that for a class of ''semifrustrated'' systems [Heisenberg models with ferromagnetic couplings $J_z(r) < 0$ along the z axis and antiferromagnetic couplings $J_{xy}(r) = -J_z(r)$ in the xy plane, for arbitrary distances r], the sign problem present for algorithms operating in the z basis can be solved within a recent ''operator-loop'' formulation of the stochastic series expansion method [a cluster algorithm for sampling the diagonal matrix elements of the power series expansion of $\exp(-\beta H)$ to all orders]. The solution relies on the identification of operator loops which change the configuration sign when updated (''merons'') and is similar to the meron-cluster algorithm recently proposed by Chandrasekharan and Wiese for solving the sign problem for a class of fermion models [Phys. Rev. Lett. **83**, 3116 (1999)]. Some important expectation values, e.g., the internal energy, can be evaluated in the subspace with no merons, where the weight function is positive definite. Calculations of other expectation values require sampling of configurations with only a small number of merons (typically zero or two), with an accompanying sign problem which is not serious. We also discuss problems which arise in applying the meron concept to more general quantum spin models with frustrated interactions.

I. INTRODUCTION

Recently, there have been several significant developments of more efficient Monte Carlo methods for interacting quantum many-body systems.[1] The Trotter decomposition formula[2,3] has traditionally been used as a starting point for finite-temperature simulation algorithms, such as the worldline[3] and fermion determinant[4] methods. It introduces a systematic error that can be removed only by carrying out simulations for several different imaginary time discretizations $\Delta\tau$ and subsequently extrapolating to $\Delta\tau = 0$. Such extrapolations are not necessary with the stochastic series expansion (SSE) method,[5–7] which is based on sampling the power series expansion of $\exp(-\beta H)$ to all orders and is related to a less general method proposed much earlier by Handscomb.[8–10] Results that are exact to within statistical errors can also be directly obtained with recent worldline[11–13] and fermion determinant[14] algorithms formulated in continuous imaginary time. Even more significant are generalizations to the quantum case[15,16,12,7] of cluster algorithms developed for the classical Monte Carlo method.[17] These ''loop algorithms'' (so called because the clusters are loops on a space-time lattice) can reduce the autocorrelation times by orders of magnitude and enable highly accurate studies of systems in parameter regimes where previous algorithms encountered difficulties due to long autocorrelation and equilibration times.

In spite of these developments, the class of models which can be studied using quantum Monte Carlo methods is still severely restricted due to the ''sign problem,''[18,19] i.e., the non-positive-definiteness of the weight function that can arise in transforming a quantum problem into a form resembling a classical statistical mechanics problem. There are two classes of systems for which this issue is particularly pressing—interacting fermions in more than one dimension and quantum spin systems with frustrated interactions (in any number of dimensions). For fermions in one dimension, and hopping between nearest-neighbor sites only, the sign problem can be avoided because the fermion anticommutation relations do not come into play (other than introducing a hard-core constraint) in the one-dimensional real-space path integral. In two or more dimensions (or even in one dimension if hopping further than between nearest neighbors is included), permutations of fermions during the propagation in imaginary time leads to a mixed-sign path integral which typically cannot be efficiently evaluated using Monte Carlo methods. The sign problem can be avoided with the fermion determinant algorithm in special cases, such as the half-filled Hubbard model (because of particle-hole symmetry),[4] but in other cases simulations are restricted to high temperatures and/or small system sizes.[18] For frustrated spin systems the source of the sign problem is different. A minus sign appears for every event in the path integral in which two antiferromagnetically interacting spins are flipped.[19] This causes an overall minus sign if the total number of spin flips is odd, which can be the case, e.g., for a triangular lattice or a square lattice with both nearest- and next-nearest-neighbor interactions. Simulations of quantum spin systems are, therefore, restricted to models with no frustration (in the off-diagonal part of the Hamiltonian), such as ferromagnets, or antiferromagnets on bipartite lattices.

A promising approach to solving the sign problem was recently suggested by Chandrasekharan and Wiese.[20] They considered a system of spinless fermions on a two-dimensional square lattice within the context of the worldline loop algorithm.[15] They showed that, for this particular model and for a certain range of nearest-neighbor repulsion strengths, the properties of the loops can be used to eliminate

the sign problem. Flipping a loop can change the number of fermion permutations from odd to even, or vice versa, thereby also changing the overall sign of the configuration. Such sign-changing loops are called ''merons.'' The magnitude of the weight is not affected by flipping a meron and, therefore, all configurations with one or more merons cancel in the partition function. The subspace of zero merons is positive definite and can be sampled without a sign problem. Typical operator expectation values of interest also contain contributions from configurations with two merons which, therefore, also have to be included in the simulation and introduce a ''mild'' sign problem. The relative weights of the zero- and two-meron subspaces to be sampled can further be chosen in an optimum way using a reweighting technique, which further reduces the sign problem.

In this paper we explore an analogous method for solving the sign problem for frustrated quantum spin models. We consider the operator-loop formulation of the SSE method,[7] in which sequences of two-spin operators are sampled by forming clusters (loops) of operators that can be simultaneously updated without changes in the weight function. The updated clusters contain operators acting on the same spins, but diagonal operators may be changed to off-diagonal ones and vice versa. For a model with frustrated interactions an operator-loop update can lead to a sign change. In analogy with Chandrasekharan and Wiese[20] we will refer to such sign-changing loops as ''merons.'' The sign problem can be solved if the operator loops for a given configuration can be uniquely defined and the weight function is positive definite in the configuration subspace containing no merons. Unfortunately, we find that these criteria are in general difficult to satisfy. Operator-loop algorithms with uniquely determined loops are typically nonergodic for frustrated systems, and with supplemental local updates for ergodicity there are mixed signs in the zero-meron subspace. In fact, in such cases merons typically do not even exist, i.e., none of the operator loops can change the sign when flipped. We have found only one spin system for which the sign problem can be eliminated using merons— the Heisenberg model with ferromagnetic couplings $J_z(r)<0$ along the z axis and frustrated antiferromagnetic couplings $J_{xy}(r)=-J_z(r)$ in the plane perpendicular to this axis, i.e., the Hamiltonian

$$H=-\sum_{i,j} J_{ij}[S_i^z S_j^z-\tfrac{1}{2}(S_i^+ S_j^- + S_i^- S_j^+)], \tag{1}$$

where $J_{ij}>0$ and the range of the couplings is arbitrary. We have implemented a meron algorithm for this model on a square lattice with nearest- and next-nearest-neighbor couplings $J(1)$ and $J(\sqrt{2})$. Standard algorithms for this model have a severe sign problem when using the z axis as the quantization axis, however, it can be avoided by a simple rotation to the x representation. Using the SSE algorithm and the meron concept, the sign problem can be eliminated also in the z representation. With both representations accessible in simulations, correlation functions both parallel and perpendicular to the z direction can be easily evaluated.

The model, Eq. (1), can be mapped onto a hard-core boson model with attractive interactions and frustrated hopping. Frustration in the potential energy has been investigated in this context as a possible mechanism to render a disordered bosonic ground state.[21] Frustration in the hopping [the xy term in Eq. (1)] should decrease the tendency to forming off-diagonal long-range order and could then lead to a normal fluid (nonsuperfluid). However, the highly symmetric case considered here has a trivial, ordered ground state; the fully polarized ferromagnetic state (corresponding to a completely filled lattice of hard-core bosons; a trivial case of normal solid). Effects of frustration only come into play at finite temperature, where the model is different from the corresponding isotropic ferromagnet (on nonfrustrated, bipartite lattices the two models are equivalent, since the sign of the xy term can be switched by a spin rotation on one of the sublattices).

Although we have not been able to solve the sign problem for other cases, such as the Heisenberg model with completely antiferromagnetic interactions [$J_z(1)=J_{xy}(1)>0$ and $J_z(\sqrt{2})=J_{xy}(\sqrt{2})>0$], our work nevertheless gives some further insights into the meron concept and what is required in order to solve the sign problem for arbitrary couplings.

The outline of the rest of the paper is the following: In Sec. II we review the basics of the stochastic series expansion method and discuss operator-loop updating schemes for both ferromagnetic and antiferromagnetic couplings. In Sec. III we present the solution of the sign problem for the $J_z(r)=-J_{xy}(r)$ model. The reweighting technique is analyzed in some detail in Sec. IV. In Sec. V we discuss some simulation results for the semifrustrated model and make comparisons with the isotropic Heisenberg ferromagnet. We summarize our work in Sec. VI.

II. OPERATOR-LOOP ALGORITHM

In this section we first briefly review the expansion underlying the SSE method and then discuss the operator-loop updates used to efficiently sample the expansion. We here assume a nonfrustrated case and postpone the discussion of the sign problem for frustrated models to Sec. III. For definiteness we consider the $S=1/2$ Heisenberg model

$$H=\pm J\sum_{\langle i,j\rangle} S_i\cdot S_j, \tag{2}$$

where $\langle ij\rangle$ denotes a pair of nearest-neighbor spins on a cubic lattice (in an arbitrary number of dimensions), and $J>0$. Depending on the sign, the model is an antiferromagnet $(+)$ or a ferromagnet $(-)$. To construct the SSE configuration space the Hamiltonian is rewritten as a sum of diagonal and off-diagonal operators

$$H=-\frac{J}{2}\sum_{b=1}^{M}(H_{1,b}\mp H_{2,b})+C, \tag{3}$$

where the index b denotes an interacting spin pair (bond) $\langle i(b),j(b)\rangle$ and C is an irrelevant constant equal to $MJ/4$, where M is the total number of pairs of interacting spins. The bond-indexed operators are given by

$$H_{1,b}=2(\tfrac{1}{4}\mp S_{i(b)}^z S_{j(b)}^z), \tag{4}$$

$$H_{2,b}=S^+_{i(b)}S^-_{j(b)}+S^-_{i(b)}S^+_{j(b)}. \quad (5)$$

Note that the eigenvalues of both the diagonal ($H_{1,b}$) and the off-diagonal ($H_{2,b}$) operators are 0 and 1, both for the antiferromagnet and the ferromagnet. The partition function $Z=\mathrm{Tr}\{\exp(-\beta H)\}$ is expanded as[5]

$$Z=\sum_\alpha \sum_{n=0}^{\infty} \frac{(-\beta)^n}{n!}\langle\alpha|H^n|\alpha\rangle, \quad (6)$$

in the basis $\{|\alpha\rangle\}=\{|S^z_1,S^z_2,\ldots,S^N_z\rangle\}$, where N is the number of spins. Terms of order greater than $n\sim N\beta$ give an exponentially vanishing contribution and for the purpose of a stochastic sampling the expansion can, therefore, be truncated at some $n=L$ of this order without loss of accuracy (see, e.g., Ref. 6 for details on how to choose a sufficiently high truncation power). Additional unit operators $H_{0,0}\equiv 1$ are introduced to rewrite Eq. (6) as

$$Z=\sum_\alpha \sum_{S_L} \frac{(\mp 1)^{n_2}(J\beta)^n(L-n)!}{2^n L!}\left\langle \alpha\left|\prod_{i=1}^{L} H_{a_i,b_i}\right|\alpha\right\rangle, \quad (7)$$

where S_L denotes a sequence of operator indices

$$S_L=(a_1,b_1)_1,(a_2,b_2)_2,\ldots,(a_L,b_L)_L, \quad (8)$$

with $a_i\in\{1,2\}$ and $b_i\in\{1,\ldots,M\}$, or $(a_i,b_i)=(0,0)$. The number of non-(0,0) elements in S_L is denoted n, while n_2 denotes the number of off-diagonal operators in the sequence. Note that since the expectation value in Eq. (7) is always equal to zero or one, the sign of a term is negative only if n_2 is odd. This sign problem occurs (only) when frustration is present and is the main topic of this paper. However, for the discussion of the sampling procedures, in this section we assume a positive definite expansion. We introduce the notation $|\alpha(p)\rangle$ for a propagated state

$$|\alpha(p)\rangle=\prod_{i=1}^{p} H_{a_i,b_i}|\alpha\rangle, \quad (9)$$

where for an allowed configuration $|\alpha(0)\rangle=|\alpha(L)\rangle=|\alpha\rangle$ and the weight function corresponding to Eq. (7) is given by

$$W(\alpha,S_L)=\frac{(J\beta)^n(L-n)!}{2^n L!}. \quad (10)$$

Having established the framework we will proceed to describe the procedures for importance sampling of the terms (α,S_L) according to the weight (10). The initial state can be a sequence of the form $(0,0)_1,(0,0)_2,\ldots,(0,0)_L$ (subscripts on the index pairs will sometimes be used to denote the position in S_L) and a random state $|\alpha\rangle$. An ergodic procedure for sampling the terms is achieved using two types of basic updates; a simple substitution of single diagonal operators and the operator-loop update which involves simultaneous updates of a number (in principle, varying between 1 and n) of diagonal and off-diagonal operators.

The diagonal update is carried out by traversing the operator-index sequence S_L from beginning ($p=1$) to end ($p=L$). Operator substitutions of the form $(0,0)_p\leftrightarrow(1,b)_p$ are attempted where possible, while the stored state $|\alpha\rangle$ is updated every time an off-diagonal operator is encountered so that the state $|\alpha(p)\rangle$ is available when needed. With the weight function (10) detailed balance can be seen to be satisfied if the acceptance probabilities are taken to be

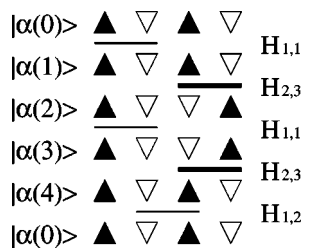

FIG. 1. Representation of a term in the SSE expansion of a four-site antiferromagnet. Up and down spins are represented as solid and open triangles, respectively. The horizontal bars indicate the presence of diagonal (thin lines) and off-diagonal (thick lines) operators.

$$P[(0,0)_p\to(1,b)_p]=\frac{MJ\beta\langle\alpha_b(p)|H_{1,b}|\alpha_b(p)\rangle}{L-n}, \quad (11)$$

$$P[(1,b)_p\to(0,0)_p]=\frac{L-n+1}{MJ\beta\langle\alpha_b(p)|H_{1,b}|\alpha_b(p)\rangle}. \quad (12)$$

Note that the diagonal update changes the expansion power n by ± 1. Off-diagonal operators cannot be introduced one-by-one because of the periodicity condition $|\alpha(L)\rangle=|\alpha(0)\rangle$. Local updates involving two operators can be used for this purpose,[6] but are more complicated and far less efficient than the operator-loop update,[7] which is discussed next.

We use a largely pictorial description of the operator loops. First we consider the antiferromagnet. Note that in this case the only nonzero matrix elements of the bond operators are

$$\langle\downarrow\uparrow|H_1|\downarrow\uparrow\rangle=\langle\uparrow\downarrow|H_1|\uparrow\downarrow\rangle=1,$$
$$\langle\downarrow\uparrow|H_2|\uparrow\downarrow\rangle=\langle\uparrow\downarrow|H_2|\downarrow\uparrow\rangle=1, \quad (13)$$

i.e., they can act only on antiparallel spins. An example of a term in the expansion for a four-site antiferromagnet is depicted in Fig. 1. This representation makes evident the close relationship between the SSE expansion and the Euclidean path integral. An imaginary time separation τ corresponds to a distribution of propagations Δp between states, centered around $\Delta p=(\tau/\beta)n$.[5,13] We will for convenience here refer to the propagation as the time dimension.

The general idea[15] behind the loop update is to flip a cluster of spins in the configuration in such a way that the weight is not changed. With the SSE method there will also have to be changes made to the operators acting on the spins, since otherwise operators H_1 or H_2 may act on parallel spins, resulting in zero-valued matrix elements. Since one of the states $|\alpha(p)\rangle$ and the operator sequence S_L uniquely define the whole spin configuration, the SSE loops are in practice treated as loops of operators, the exact meaning of which will be made clear below.

Consider one of the operators $H_{1,1}$ in Fig. 1. It can be depicted as a ''vertex'' with four legs associated with spin states $\downarrow$ or $\uparrow$. If we flip the upper left spin, a vanishing matrix

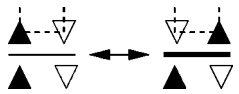

FIG. 2. Spin flip and accompanying operator exchange during a loop update for an antiferromagnet. The dashed line indicates part of the loop.

element results. But if we flip both upper (or lower) spins and also change the operator type to off-diagonal $H_{2,1}$, an allowed matrix element is generated; see Fig. 2. Using this idea we can form a cluster of spins by choosing a random spin $S_i^z(p)$ in the configuration and traversing up or down until we encounter an operator (bond) acting on that spin, then switch to the second spin of the bond and change the direction of traversing the list. Eventually we will necessarily arrive back at the initial starting point, whereupon a closed loop has formed. All the spins on this loop can be flipped if the operators encountered are also switched $[(1,b)\leftrightarrow(2,b)]$. Note that the same operator can be encountered twice, which results in no net change of operator type (but the spins at all four vertex legs are flipped).

The whole configuration can be uniquely divided up into a set of loops, so that each spin belongs to one and only one cluster; see Fig. 3, where our example configuration has been divided up into three clusters. All loops can be flipped independently with probability 1/2—in Fig. 3 we depict the result of flipping the largest loop of the example configuration. A full operator-loop update amounts to dividing up the configuration into all of its loops which are flipped with probability 1/2. The (random) decision of whether or not to flip a loop can be made before the loop is constructed, so that each loop has to be traversed only once. Spin ''lines'' $S_i^z(p)$, $p=0,\ldots,n$, which are not acted upon by any of the operators in S_L will not be included in any of the operator loops. They correspond to ''free'' spins which can be flipped with probability 1/2. Such a line can also be considered a loop, and then it will always be true that every spin $S_i^z(p)$ belongs to one loop. Free spins appear frequently at high temperatures, when the total number of operators $n\lesssim N$, but are rare at low temperatures.

Note that the spin states at the four legs of the operator vertices completely determine the full spin configuration, except for free spins that happen not to be acted upon by any of

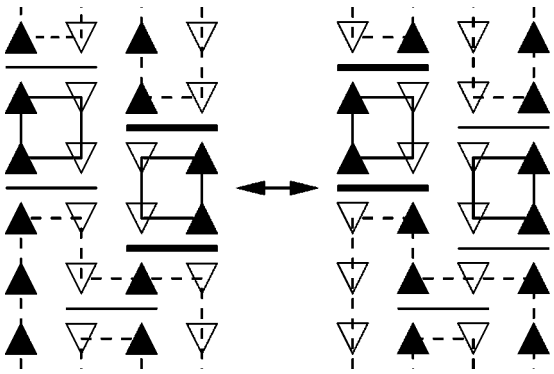

FIG. 3. The SSE space-time configuration of Fig. 1 is uniquely divided up into loops (left). The right-hand configuration results from flipping the loop indicated by the dashed line. Note the periodic boundary conditions in the vertical (''time'') direction.

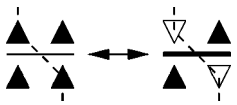

FIG. 4. Spin flip and accompanying operator exchange during a loop update for a ferromagnet. The dashed line indicates part of the loop.

the operators in S_L. Hence, the operator-loop update can be carried out using only a linked list of of operators, i.e., an array of vertices with four spin states and associated pointers to the ''previous'' and ''next'' vertices associated with the same spin. The storage requirements and the number of operations needed for carrying out a full operator-loop update then scale as $\sim N\beta$ instead of $\sim N^2\beta$ if the full spin configuration were to be used.

In a simulation we first make a full cycle of diagonal updates in the sequence S_L and then create the linked list of vertices in which the operator-loop updates are carried out. The vertex list is then mapped back onto the sequence S_L and the state $|\alpha(0)\rangle$. Alternatively, the linked list can be updated simultaneously with each diagonal operator substitution, so that it does not have to be recreated for each Monte Carlo step—depending on the model studied there may be significant differences in execution time between the two approaches.

For the ferromagnet we can construct the loops in a similar manner, but the nonzero matrix elements are now

$$\langle\downarrow\downarrow|H_1|\downarrow\downarrow\rangle=\langle\uparrow\uparrow|H_1|\uparrow\uparrow\rangle=1,$$
$$\langle\downarrow\uparrow|H_2|\uparrow\downarrow\rangle=\langle\uparrow\downarrow|H_2|\downarrow\uparrow\rangle=1, \tag{14}$$

i.e., the off-diagonal operators act only on antiparallel spins, as before, whereas the diagonal ones can act only on parallel configurations. This implies qualitative changes in the structure of the loops, as depicted in Fig. 4. If we again consider an operator H_1 and flip the upper left spin, we note that we need to flip the lower right spin and change the operator to H_2, Hence, instead of changing the direction of traversing the configuration every time an operator is encountered we now continue in the same direction after switching to the second spin of the bond. Any configuration can still be uniquely divided up into loops that can be flipped with probability 1/2. An example of a ferromagnetic configuration with its loops is shown in Fig. 5.

Note that since the loops for the ferromagnet never change direction as they go through the lattice, every single loop has to traverse each state $|\alpha(p)\rangle$ at least once. It follows that the number of sites N is an upper bound of the number of loops. The antiferromagnetic loops, on the other hand, traverse the lattice in both directions and the number of loops is, therefore, instead limited by the total number of operators $n\sim N\beta$. As a consequence of the change of direction, for the antiferromagnet the linked list of vertices must to be bidirectional, whereas for the ferromagnet it is sufficient to keep a singly directional list.

The diagonal and operator-loop updates satisfy detailed balance and the combination of them leads to ergodic sampling for a ferromagnet on any lattice, and for antiferromagnets on bipartite lattices—for frustrated antiferromagnets there are complications, in addition to the sign problem,

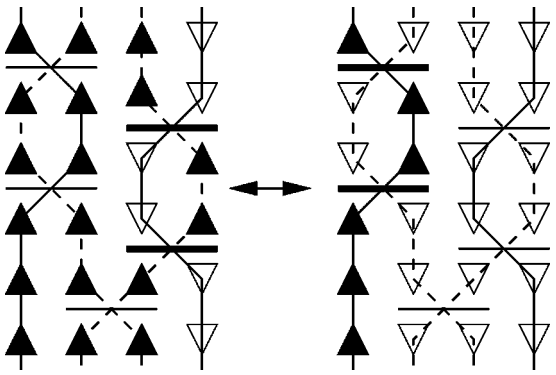

FIG. 5. SSE space-time configurations uniquely divided into loops for the case of a ferromagnet. The left- and right-hand configurations differ by flipping the loop indicated by a dashed line.

which will be discussed further in the next section. The operator-loop sampling is highly efficient, with integrated autocorrelation times typically less than one updating cycle (Monte Carlo step).

The loop construction described here relies on the rotational invariance of the models, i.e., the fact that both the diagonal and off-diagonal matrix elements in Eqs. (13) and (14) are equal to one. For a general anisotropic case, or in the presence of fields, the loops will lead to weight changes when flipped and must then be assigned *a posteriori* acceptance probabilities which typically become small for large lattices at low temperatures.[22] Other types of loops avoiding this problem have been proposed,[7] but will not be discussed here.

III. THE SIGN PROBLEM

The notorious sign problem arises in stochastic sampling when the function used to weight the different configurations is not positive definite. A typical quantity that can be calculated by Monte Carlo methods (importance sampling) is of the form

$$\langle A\rangle = \frac{\sum_i A(x_i)W(x_i)}{\sum_i W(x_i)} = \langle A(x)\rangle_W, \tag{15}$$

where W is the weight function and $A(x)$ is the estimator corresponding to the measured quantity, which both depend on the general coordinate x of the configuration space sampled. When the coordinates are sampled according to relative weight, the desired quantity is simply the arithmetic average of the estimator $A(x)$, as indicated by the notation $\langle A(x)\rangle_W$ above. If the weight function is not positive definite, the sampling can be done using the absolute value of the weight, and the expectation value can be calculated according to

$$\langle A\rangle = \frac{\langle A(x)s(x)\rangle_{|W|}}{\langle s(x)\rangle_{|W|}}, \tag{16}$$

where $s(x)$ equals ± 1, depending on whether the sign of the weight function is positive or negative. For most models, where a sign problem is present, the average sign $\langle s(x)\rangle_{|W|}$ decreases exponentially to zero as a function of inverse temperature and system size, and the relative statistical errors of calculated quantities increase exponentially.

A meron-cluster solution to the sign problem using loop updates of fermion world-line configurations was recently proposed by Chandrasekharan and Wiese.[20] This approach is based on the idea that if it is possible to map every configuration with negative weight uniquely to a corresponding configuration with equal weight magnitude but opposite sign, then the partition function can be sampled without a sign problem simply by not including any configuration which is a member of such a canceling pair. In the meron-cluster algorithm, flipping a loop of spins can lead to a sign change without change in the magnitude of the weight, and such a ''meron'' hence identifies a canceling pair of configurations. Here we will present a similar approach within the SSE operator-loop method for frustrated quantum spins.

Let us consider the Heisenberg antiferromagnet discussed in the previous section. From Eq. (7) we see that a configuration has negative weight if the total number n_2 of off-diagonal operators is odd. This can only be the case on frustrated lattices. As described in the previous section, any SSE configuration can be divided up uniquely into a number of loops. Flipping a loop interchanges the diagonal and off-diagonal operators, but leaves the total number of operators unchanged. It follows that the sign will change if and only if a loop passing through an odd number of operators is flipped (two passes through the same operator is counted as two operators). Since the total weight remains unchanged we have thus found the desired mapping between positive and negative configurations (assuming that there exist loops which change the sign when flipped, which in fact is not always the case). In analogy with previous work we call such a sign-flipping loop a ''meron.'' Let us now see how we can use this concept to calculate observables.

As in Ref. 20 we consider improved estimators that averages over all loop configurations. Denote the number of loops in the system N_L. Since each loop can be in one of two states there is a total of 2^{N_L} configurations that can be reached by flipping all combinations of the loops present. The improved estimate therefore takes the form

$$\langle A\rangle = \frac{\langle\langle A(x)s(x)\rangle\rangle_{|W|}}{\langle\langle s(x)\rangle\rangle_{|W|}}, \tag{17}$$

where the double brackets denote an average over all the loop states for each generated SSE configuration, e.g.,

$$\langle\langle s(x)\rangle\rangle = \left\langle \frac{1}{2^{N_L}} \sum_{l=1}^{2^{N_L}} s(x_l) \right\rangle. \tag{18}$$

The general coordinate x here refers to the SSE configuration space (α, S_L) and x_l refers to one out of the 2^{N_L} possible outcomes of ''flipping'' a number of loops.

Let us consider this average. Denote the state of a loop with δ, with two possible ''orientations'' $\delta \in \{\uparrow,\downarrow\}$. Since flipping one loop does not affect any other loops (in terms of their paths taken), the sign of a configuration factors according to

$$s(\delta_1,\delta_2,\ldots,\delta_{N_L})=\prod_{i=1}^{N_L} s(\delta_i), \tag{19}$$

where $s(\delta)=\pm s(\overline{\delta})$, where $\overline{\delta}$ denotes a flipped loop, and the sign is negative for merons and positive otherwise. Since flipping any meron leads to two terms that cancel, it follows that

$$\frac{1}{2^{N_L}}\sum_{l=1}^{2^{N_L}} s(x_l)=\pm\,\delta_{n_M,0}, \tag{20}$$

where n_M denotes the total number of merons. The sign in front of the delta function is the ''inherent'' sign of the configuration, independent of the loop orientation when there are no merons present. This sign has to be positive for the meron solution to be applicable in practice, and then the partition function can be sampled in the positive definite subspace of configurations with no merons.

Having found an expression for the denominator in Eq. (17) we need to consider the numerator for cases of interest. SSE estimators for a number of important operators have been discussed, e.g., in Ref. 6. The internal energy is given by

$$E=-\frac{1}{\beta}\langle n\rangle_W, \tag{21}$$

where n denotes the total number of operators in the sequence S_L. This number is not affected by the loop updates, and hence it follows that

$$E=-\frac{1}{\beta}\frac{\langle\langle n(x)s(x)\rangle\rangle_{|W|}}{\langle\langle s(x)\rangle\rangle_{|W|}}=-\frac{1}{\beta}\frac{\langle n(x)\,\delta_{n_M,0}\rangle_{|W|}}{\langle\,\delta_{n_M,0}\rangle_{|W|}}. \tag{22}$$

Assuming that this sector has positive definite weight we have therefore completely eliminated the sign problem by restricting the simulation to the zero-meron sector. The energy is then simply given by

$$E=-\frac{\langle n(x^0)\rangle_W}{\beta}, \tag{23}$$

where the superscript 0 indicates the restriction of the simulation to the zero-meron sector.

Next we will consider the magnetic susceptibility,

$$\chi=\frac{\beta}{N}\left\langle\left(\sum_i S_i^z\right)^2\right\rangle=\frac{\beta}{N}\langle M^2\rangle. \tag{24}$$

Since M is conserved by the Hamiltonian its value is the same in all propagated states; $M(p)=M(0)\equiv M, p=1,\ldots,n$. In a configuration uniquely divided up into loops, every spin $S_i^z(p)$ belongs to one and only one loop, if we count as loops also all ''lines'' of free spins, i.e., the spins $S_i^z(p)$, $p=1,\ldots,n$ for all sites i which are not associated with any operator in the sequence (and therefore can be flipped). It follows that the change in $M(p)$ when flipping a loop must be the same for all p, and hence only loops that go through all states $|\alpha(p)\rangle$ (at least once) can change M when flipped. We can, therefore, introduce a loop magnetization m_L, which is simply equal to the sum of the spins traversed by the loop for an arbitrary $|\alpha(p)\rangle$. In the estimator (17) corresponding to the susceptibility the numerator can hence be written as

$$\left\langle\frac{1}{2^{N_L}}\sum_{l=1}^{2^{N_L}}[m_1(x_l)+\ldots+m_{N_L}(x_l)]^2 s(x_l)\right\rangle, \tag{25}$$

The magnetization on a loop always changes sign when a loop is flipped; the overall sign $s(x_l)$ only changes sign when a meron is flipped. Therefore, in summing over all loops in (25), a nonzero value results only if the configuration has zero or two merons. The full susceptibility estimator therefore takes the form

$$\chi=\frac{\langle\Sigma_{l=1}^{N_L}|m_l|^2\delta_{n_M,0}+2|m_{M_1}||m_{M_2}|\delta_{n_M,2}\rangle}{\langle\,\delta_{n_M,0}\rangle}, \tag{26}$$

where M_1 and M_2 are the indices of the loops corresponding to merons in a two-meron configuration. Here we have assumed that all non-meron loop signs in Eq. (19) are positive and that $m_{M_1}m_{M_2}\geqslant 0$ when the two-meron sign product is positive (the latter assumption is not necessary but is typically true in cases where the first condition holds). Hence, unlike in the case of the total energy, the sign problem has here not been completely eliminated, since the zero- and two-meron configuration contribute 1 and 0, respectively, to the average sign. When the SSE configuration volume V grows the relative weight of the zero-meron sector should diminish, leading to a decreasing average sign. Chandrasekharan and Wiese found that the statistical fluctuation in the improved susceptibility estimator increases quadratically with $N\beta$, i.e., much slower than the conventional exponential increase. They also argued that this remaining sign problem can be solved by reweighting the zero- and two-meron sectors with external weight factors $w(0)$ and $w(2)$. This changes the above formula to

$$\chi=\frac{\langle\Sigma_{l=1}^{N_L}|m_l|^2\delta_{n_M,0}w(2)+2|m_{M_1}||m_{M_2}|\delta_{n_m,2}w(0)\rangle}{\langle\,\delta_{n_M,0}w(2)\rangle} \tag{27}$$

In the next section we will say more about reweighting.

As we have shown above, the meron concept within the SSE method formally leads to exactly the same equations as in the world-line simulations of fermion systems considered in Ref. 20. The difference is only in the structure of the meron itself; the fermionic meron changes the number of particle permutations from even to odd, or vice versa, whereas the SSE meron in the case of a frustrated spin system instead changes the number of antiferromagnetic spin flips from even to odd or vice versa. Applying the SSE operator-loop algorithm to a fermion system would lead to merons of exactly the same kind as those existing within the world-line framework, and, conversely, applying a world-line loop algorithm to a frustrated spin system should lead to merons similar to those discussed here (there are no diagonal operators in the world-line configurations, but spin flip events correspond to the SSE off-diagonal operators and can change from even to odd, or vice versa, in loop updates). These similarities are not surprising, considering the close relationship between the SSE expansion and the Euclidean path integral.[13]

Now consider the application of the above ideas to the Heisenberg model on a square lattice with nearest- and next-nearest-neighbor couplings $J(1)>0$ and $J(\sqrt{2})>0$ (antifer-

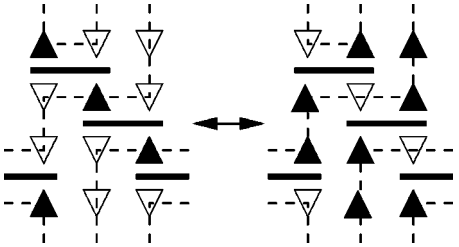

FIG. 6. Three off-diagonal operators acting on a triangle of spins. The left- and right-hand configurations differ by flipping the loop indicated by a dashed line. Note the periodic boundary conditions.

romagnetic). This model has a sign problem since the total number n_2 of spin-flipping operators in a configuration can be odd, e.g., three operators on a triangle of spins, as shown in Fig. 6. Already this simple example illustrates that the operator-loop algorithm discussed above does not sample the full configuration space and that the meron concept therefore cannot be applied to solving the sign problem. Since all three bonds are antiferromagnetic, a loop will change direction every time an operator is encountered. In order for the loop to close, it therefore has to pass through an even number of operators and hence flipping the loop cannot change the number n_2 of off-diagonal operators from odd to even, or vice versa. This is illustrated in Fig. 6, where the only effect of flipping the single loop in the system is to flip all the spins, with the operators remaining unchanged. Hence, merons do not even exist within the operator-loop algorithm for this model, and the sampling is nonergodic. A local update can, in principle, be used in combination with the operator loops in order to make the sampling ergodic. However, a configuration can then have a negative sign (of which Fig. 6 is an example) even though there are no merons present. The principal requirement of positive definiteness in the zero-meron subspace (which in this case is the full space) is hence not fulfilled. A similar problem seems to affect all models with frustration in all of the spin components. It is possible that some other way of constructing the loops could remedy this, e.g., by switching to some other, nontrivial basis in which the SSE expansion could be carried out. Other ways proposed for constructing loops in the standard basis considered here remedy the ergodicity problem but do not uniquely define the set of loops[7] and can therefore not easily be used with the meron concept.

We have found one class of spin models for which the meron ideas can be successfully applied to solve the sign problem: Heisenberg models which are antiferromagnetic in the xy plane but ferromagnetic along the z axis., i.e., the ''semifrustrated'' model (1), which can be written as

$$H=-\sum_{b=1}^{M}\frac{J_b}{2}(H_{1,b}-H_{2,b})+C, \tag{28}$$

where the bond-indexed operators are given by

$$H_{1,b}=2(\tfrac{1}{4}+S^z_{i(b)}S^z_{j(b)}), \tag{29}$$

$$H_{2,b}=S^+_{i(b)}S^-_{j(b)}+S^-_{i(b)}S^+_{j(b)}. \tag{30}$$

On a nonfrustrated lattice this model is equivalent to an isotropic Heisenberg ferromagnet, since n_2 is always even and the sign in front of the operators $H_{2,b}$ in Eq. (28) is irrelevant as $(-1)^{n_2}=1$ in Eq. (7)—the sign can also be transformed away by a spin rotation on one of the two sublattices. On a frustrated lattice, on the other hand, n_2 can be odd (the lattice is no longer bipartite so that the transformation mentioned above does not remove all signs), and the system is no longer equivalent to the isotropic ferromagnet. The model has a classical twofold degenerate ferromagnetic ground state, but at finite temperatures the transverse spin components are frustrated, and the behavior will be different from the isotropic ferromagnet. When simulated in the z basis using standard algorithms the semifrustrated model has a severe sign problem, but the zero-meron sector is positive definite and the SSE meron solution can be applied. The structure of the operator loops is the same as for the ferromagnet and the loop algorithm is therefore ergodic for any lattice and range of the interaction. We have used this model to explore the properties of the meron method.

The meron solution can be implemented in several different ways and we briefly describe how it was done in this work: During the sequential diagonal updates the linked list, representing the loop structure, is updated simultaneously with each accepted diagonal update. The loops are numbered and information is stored on whether each loop is a meron or not. During an attempted diagonal update only the loops directly affected by the operator substitution are updated. This permits easy and fast checking of whether the number of merons in the system has changed or not. If the new number of merons is different from zero or two the update is rejected, whereas if the number of merons changes from i to j it is accepted with probability $w(j)/w(i)$, where $i,j\in\{0,2\}$, and $w(i)$ is the reweighting factor assigned to meron sector i. The number of operations needed for carrying out a full operator-loop update now depends on the number of operators in each loop. If each loop passes only once through the system in the imaginary time direction, the scaling will change from βN to $\beta^2 N$. If a few large loops dominate, the scaling will assume the worst case form $(\beta N)^2$. In most cases of interest the scaling is likely to be somewhere between these two limits.

Note that the sign problem for the semifrustrated model can also be very easily transformed away by rotating the ferromagnetic component to the y direction. The Hamiltonian then takes the form

$$H=-\frac{J}{2}\sum_{b=1}^{M}(H'_{1,b}+H'_{2,b})+C, \tag{31}$$

where the bond-indexed operators are given by

$$H'_{1,b}=2(\tfrac{1}{4}-S^z_{i(b)}S^z_{j(b)}), \tag{32}$$

$$H'_{2,b}=S^+_{i(b)}S^+_{j(b)}+S^-_{i(b)}S^-_{j(b)}, \tag{33}$$

and the fundamental spin-flips and operator exchange during a loop update is shown in Fig. 7. Being able to work in both bases we can easily measure all components of the susceptibility. Our main motivation for studying this model is to illustrate how the sign problem can be removed in the z basis. Nevertheless, we will also show some results calculated in the x basis.

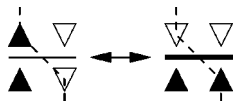

FIG. 7. Spin flip and the accompanying operator exchange during a loop update for model with a ferromagnetic x component, but antiferromagnetic y and z components. The dashed line indicates part of the loop.

IV. REWEIGHTING

An important technical aspect of the meron solution is the reweighting of the zero- and two-meron sectors, which was briefly mentioned in the previous section. Equation (27) gives the correct estimator for the susceptibility after reweighting, but it gives no information on how to do the reweighting in practice. How to determine the optimal reweighting and whether reweighting changes the scaling of the relative error are important questions to be considered in this section.

As a first example of how reweighting affects the statistics of a simulation we will discuss a simple random process. Consider a random variable n, which can take two different values, 0 or 2. Let W_0 and W_2 designate the probability for these two outcomes. The expected fractions and standard deviations of these outcomes from N random selections are given by

$$\langle \delta_{n,0} \rangle = W_0 \pm \frac{\sqrt{W_0 W_2}}{\sqrt{N}}, \tag{34}$$

$$\langle \delta_{n,2} \rangle = W_2 \pm \frac{\sqrt{W_0 W_2}}{\sqrt{N}}. \tag{35}$$

We consider an expectation value of a form similar to the susceptibility, Eq. (26);

$$\langle f \rangle = \frac{\langle \delta_{n,0} + \delta_{n,2} \rangle}{\langle \delta_{n,0} \rangle} = \frac{1}{W_0} \pm \frac{1}{W_0} \sqrt{\frac{W_2}{W_0}} \frac{1}{\sqrt{N}}, \tag{36}$$

with a relative standard deviation

$$\frac{\sigma_f}{f} = \sqrt{\frac{W_2}{W_0}} \frac{1}{\sqrt{N}}. \tag{37}$$

This formula becomes valid for large N, when the standard deviation is small. As W_0 decreases the standard deviation increases and we will consider whether reweighting can help in this situation. The two outcomes can be reweighted by assigning an additional weight W to the $n=0$ outcome such that a transition from $n=0$ to $n=2$ is accepted with probability $1/W$, while a transition from $n=2$ to $n=0$ is always accepted. After such a reweighting the probabilities of obtaining $n=0$ and $n=2$ are given by

$$W_0' = \frac{W_0 W}{W_0 W + W_2}, \tag{38}$$

$$W_2' = \frac{W_2}{W_0 W + W_2}, \tag{39}$$

and f is given by

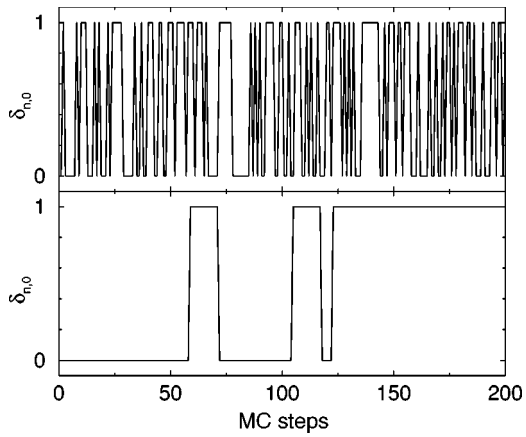

FIG. 8. Fluctuations of n during a random process with two outcomes ($n=0,2$). The upper graph shows results for $W_0=0.5$ and $W_2=0.5$, while in the lower graph $W_0=0.01$ and $W_2=0.99$ and a reweighting factor $W=99$ is used (resulting in $W_0'=W_2'=0.5$).

$$\langle f \rangle = \frac{\langle \delta_{n,0} + W \delta_{n,2} \rangle}{\langle \delta_{n,0} \rangle}. \tag{40}$$

When calculating the standard deviation for this case we have to be careful since the reweighting introduces correlations into the system. This is clearly visualized in Fig. 8, where in the upper graph a series of independent outcomes with equal probability ($W_0=W_2=0.5$) are shown, while in the lower graph a case with $W_0=0.01$ is shown with a reweighting factor of $W=99$ (leading to $W_0'=W_2'=0.5$).

Let us now calculate the standard deviation and its statistical error for this case. In a standard MC simulation one usually wants to calculate the average and the standard deviation of the average for some quantity x. This is typically achieved by dividing the run into a number of bins, N, and saving the average of x for each bin. If the bins are statistically independent the final average and standard deviation can be calculated according to

$$\langle x \rangle = \frac{1}{N} \sum_{i=1}^{N} x_i \tag{41}$$

and

$$\sigma_{\langle x \rangle} = \sqrt{\frac{\langle x^2 \rangle - \langle x \rangle^2}{N}}. \tag{42}$$

When studying the behavior of the standard deviation itself, we also want to obtain an estimate of the accuracy of the standard deviation. This can be done by dividing the N bins into M sets containing N/M bins each. For each set a standard deviation σ_x can be calculated according to

$$\sigma_x = \sqrt{\langle x^2 \rangle - \langle x \rangle^2}, \tag{43}$$

where the brackets denote an average of the N/M bins within the set. The final standard deviation and its statistical fluctuation are then given by

$$\langle \sigma_x \rangle = \frac{1}{M} \sum_{i=1}^{M} \sigma_{xi} \tag{44}$$

and

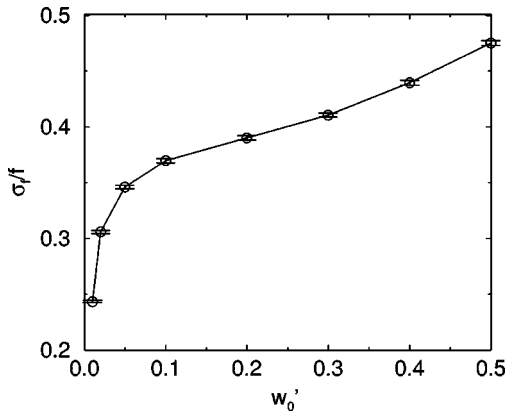

FIG. 9. The relative standard deviation of f as a function of W_0'. Calculations are performed over bins containing $N_{\mathrm{bin}}=2000$ MC steps.

$$\sigma_{\langle\sigma_x\rangle}=\sqrt{\frac{\langle\sigma_x^2\rangle-\langle\sigma_x\rangle^2}{M}}. \tag{45}$$

Equation (44) represents the standard deviation of the distribution of the binned values x, and not the standard deviation of an average of these. It does not decrease as the number of bins N is increased, but it is dependent on the number of MC steps in each bin, N_{bin}, and will decrease as $1/\sqrt{N_{\mathrm{bin}}}$. Hence it is important to state the number of MC steps in the bins for which the deviation is calculated. The statistical error of this standard deviation, $\sigma_{\langle\sigma_x\rangle}$, will, on the other hand, decrease as $1/\sqrt{N}$.

In this manner we can calculate the standard deviation for f. In order to show the standard deviation as a function of the reweighted probability W_0', Eq. (38) can be inverted to express the necessary weight factor that causes the average to change from W_0 to W_0';

$$W=\frac{W_0'(1-W_0)}{W_0(1-W_0')}. \tag{46}$$

Simulation results for the standard deviation of f as a function of W_0' is shown in Fig. 9. We see that the reweighting actually increases the standard deviation. This is due to the rapidly increasing auto correlation times. The autocorrelation function

$$C_\delta(t)=\frac{\langle\delta_{n,0}(i+t)\,\delta_{n,0}(i)\rangle-\langle\delta_{n,0}(i)\rangle^2}{\langle\delta_{n,0}(i)^2\rangle-\langle\delta_{n,0}(i)\rangle^2} \tag{47}$$

is shown in Fig. 10, and one can see that the autocorrelation times (proportional to the slopes in Fig. 10) are proportional to W_0'. Notice that the longest autocorrelation times are significantly shorter than the individual bins (consisting of 2000 MC steps) used above, a criteria for the analysis to be valid. The increasing autocorrelation time can be easily understood by considering the case depicted in Fig. 8. After reweighting, the probability of a transition from $n=0$ to $n=2$ remains 0.01, while the probability of a transition from $n=2$ to $n=0$ is decreased from 0.99 to 0.01, thereby making the two

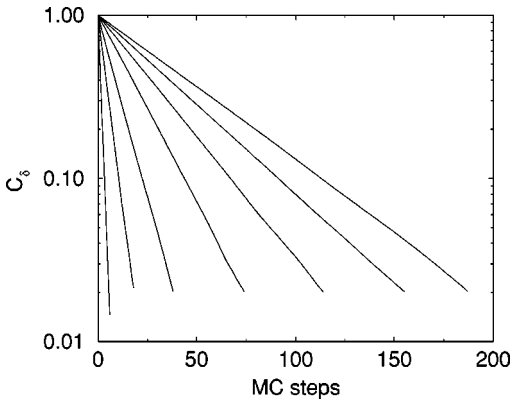

FIG. 10. Autocorrelation function, Eq. (47), as a function of W_0'. Shown are results for $W_0'=0.02$, 0.05, 0.1, 0.2, 0.3, 0.4, and 0.5 (curves left to right).

transition rates equal. The reweighting therefore decreases the transition rates between the sectors, which leads to longer autocorrelation times.

This simple example seems to indicate that reweighting does not decrease the statistical errors. However, in a standard Monte Carlo simulation the measured quantities are typically correlated even with no reweighting, and formula Eq. (27) contains measured quantities different from Eq. (36) considered above. The cost of lower transition rates between the sectors can be outweighed by a more efficient sampling of the separate sectors. Therefore, the reweighting will affect autocorrelation times differently than in the above example, and reweighting can actually decrease the standard error.[20]

Using the above technique we can study how the relative error in the susceptibility of the semifrustrated model is affected by reweighting. An initial run without reweighting has to be done first to determine the average sign $\langle\delta_{n,0}\rangle=W_0$. Thereafter, Eq. (46) can be used to determine the desired weight factors. In Fig. 11 the average sign in a simulation of the semifrustrated model with $J(1)=J(\sqrt{2})=J$ is shown as a function of lattice volume $V=L\times L$ at a temperature $T/J=1.0$. For comparison we first performed a standard simulation by sampling all meron sectors, which leads to a severe sign problem with a sign that decreases exponentially in sys-

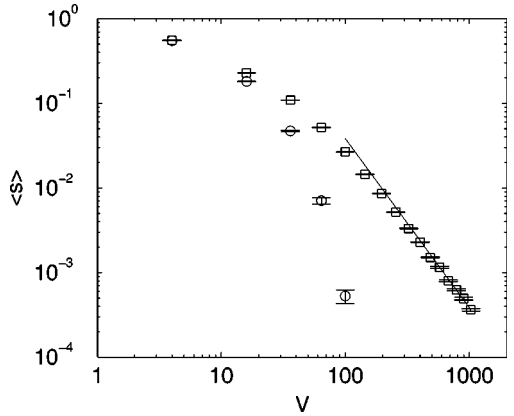

FIG. 11. The average sign as function of system volume at temperature $T/J=1$. Shown are results of an unrestricted simulation (circles), and a simulation restricted to the 0- and 2-meron sectors without reweighting (squares). The line shows a slope of -2.

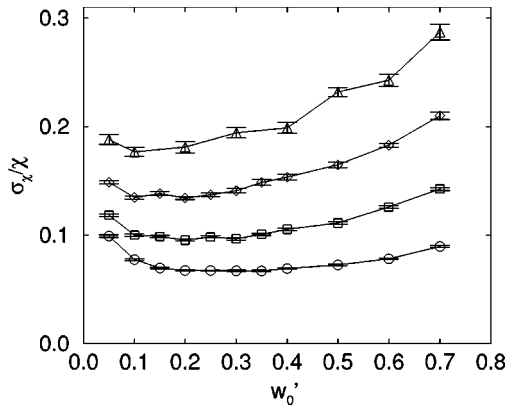

FIG. 12. Relative standard deviation of the z susceptibility of the semifrustrated model as a function of reweighting. Shown are results for systems of linear size 8 (circles), 12 (squares), 16 (diamonds), and 20 (triangles). The standard deviation is calculated for bins containing $N_{\mathrm{bin}}=10^3$ MC steps at temperature $T/J=1.0$.

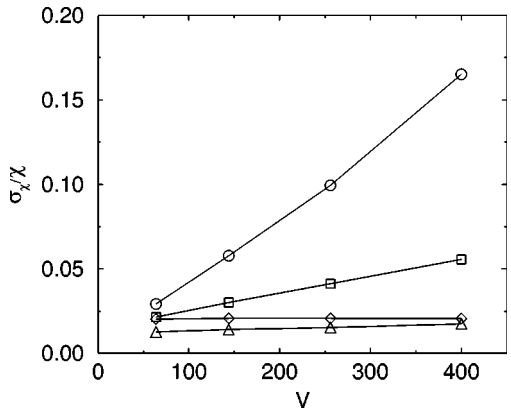

FIG. 13. The standard deviation of the susceptibility as a function of system volume V. Shown are: the z component for the semifrustrated model without (circles) and with (squares) optimal reweighting, the x component for the semifrustrated model (diamonds), and the rotationally invariant susceptibility of the ferromagnetic model (triangles). Statistical errors are smaller than symbol size.

tem volume. Next we sampled only the zero- and two-meron sectors without reweighting, which dramatically increases the average sign. The scaling changes from exponential to inverse quadratic in the volume, as can clearly be seen from the graph.

Having determined the average sign without reweighting we now use Eq. (46) to determine the desired weight factors. Figure 12 shows the standard deviation (44) of the susceptibility, calculated using bins containing 1000 MC steps. Results are shown for systems of linear size $L=8$, 12, 16, and 20 at temperature $T/J=1.0$. Reweighting clearly helps to reduce the standard deviation, and there is a definite minimum in all these curves indicating an optimal reweighting. The optimally reweighted sign always appears to be less than 0.5, and decreases with decreasing sign (and increasing volume).

Having determined that there is an optimal reweighting we will next consider whether reweighting changes the scaling with system size of the relative statistical error. Let us first consider how the standard deviation scales with no reweighting. Since the sign decreases quadratically in the volume V we can derive the scaling of the relative error in the sign, under the ideal (and typically false) assumption that individual measurements are completely independent. Using that $s=s^2$ we arrive at

$$\frac{\sigma_s}{\langle s\rangle}=\frac{\sqrt{\langle s^2\rangle-\langle s\rangle^2}}{\langle s\rangle\sqrt{N}}\sim\frac{1}{\sqrt{\langle s\rangle N}}=\frac{V}{\sqrt{N}}, \tag{48}$$

and this indicates that in this case the statistics needed increases quadratically in system volume, as also stated in Ref. 20.

In order to study the scaling, the standard deviation for bins containing $N_{\mathrm{bin}}=10^4$ MC measurements of the susceptibility is shown in Fig. 13. Four susceptibilites are shown: the z component for the semifrustrated model without and with optimal reweighting, the x component for the semifrustrated model and the rotationally invariant susceptibility of the isotropic ferromagnetic model. The two latter quantities can be obtained in simulations without sign problems, as discussed in the previous section

Let us first consider the z component of the susceptibility for the semifrustrated model without and with optimal reweighting. For *both* cases the graph suggests a linear increase in relative error. We have to keep in mind that Eq. (48) does not have to be valid, since there are autocorrelations in the simulation, and the results in Fig. 13 do not exclude that the scaling changes when approaching the thermodynamic limit (due to increasing autocorrelation times), but both results do support an approximately linear increase. It appears that the reweighting in this case changes only the prefactor of the volume scaling, but not the exponent. This seems to indicate that the reweighting has not completely eliminated the remaining sign problem (the error remains much larger than that for the ferromagnet susceptibility). It is, however, clear that the reweighting reduces the standard deviations by a significant factor. In any case, an algorithm that changes the functional dependence of the size scaling of the statistics from exponential to polynomial can be considered a solution to the problem.

The x susceptibility of the semifrustrated model, which is evaluated with an algorithm without sign problems, shows a constant standard deviation, which may be related to the fact that the susceptibility itself has converged to its thermodynamic limit for these system sizes (see next section). For the isotropic ferromagnetic model, the susceptibility still shows a linearly increasing error, but as already noted the slope is much smaller than for the semifrustrated case.

This concludes our discussion of the reweighting technique. In future work it would be interesting to explore how the optimal reweighting can be determined directly from quantities measured during one single test run, rather than by explicitly measuring the standard deviations as we have done here.

V. RESULTS

In this section we will present results for the semifrustrated and isotropic ferromagnetic models. We will demonstrate that it is feasible to obtain accurate results for large systems in the z basis by using the meron solution. The main

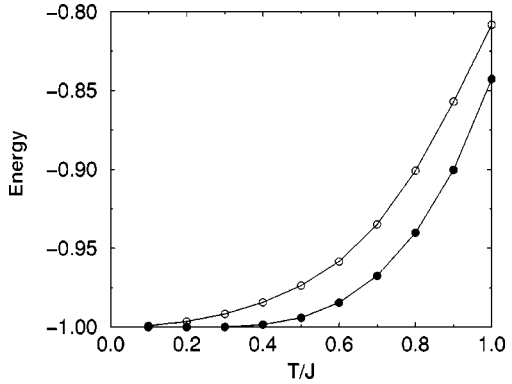

FIG. 14. Energy for the semifrustrated (filled circles) and ferromagnetic (empty circles) model, with $J(1)=J(\sqrt{2})=J$. Statistical errorbars are not visible in the plot, and the curves have converged to the thermodynamic limit.

motivation for this study is to analyze the meron solution, and we will only briefly comment on the physics of the semifrustrated model and how it differs from the isotropic ferromagnet. We will primarily consider the case with $J(1)=J(\sqrt{2})=J$. To verify the correctness of our codes we have compared simulation results with exact diagonalization data for systems with 4×4 spins.

In Fig. 14 the internal energy per spin is shown for the semifrustrated and ferromagnetic model. The statistical errorbars are smaller than the symbol size and the results have converged to the thermodynamic limit. The largest system size used had 128×128 spins. It can be seen that thermal fluctuations and finite-temperature quantum fluctuations more effectively destroy the fully ferromagnetic state for the isotropic ferromagnet than for the semifrustrated model.

The z component of the susceptibility is shown for both models in Fig. 15. The low-temperature susceptibility for finite-size systems will approach $\beta N/4$ for the semifrustrated model, and $\beta N/12$ for the ferromagnetic model (reduced by a factor 1/3 due to rotational averaging in the latter case). This can be clearly seen from Fig. 15, where the susceptibility is multiplied by temperature, so that a constant at low temperatures indicates a Curie divergence. In the thermodynamic limit the uniform susceptibility should diverge exponentially

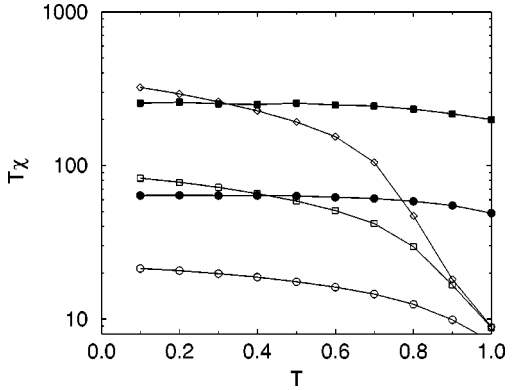

FIG. 15. The z component of the susceptibility for the semifrustrated (filled symbols) and the ferromagnetic model (empty symbols). The size effects are shown for linear system sizes $L=16$ (circles), 32 (squares), and 64 (diamonds, shown only for the ferromagnetic model). Statistical errorbars are not visible on this scale.

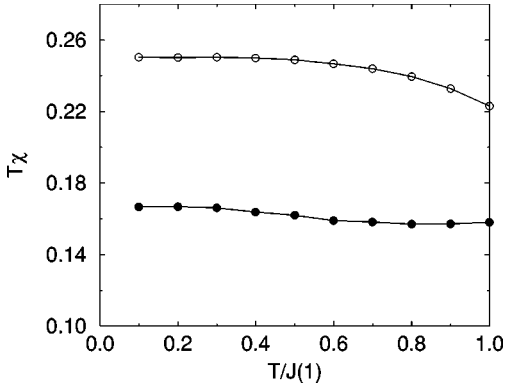

FIG. 16. The x component of the susceptibility for the semifrustrated model, with $J(\sqrt{2})=J(1)$ (empty circles) and $J(\sqrt{2})=0$ (filled circles). Statistical errorbars are not visible.

for these models, but this cannot be clearly seen in Fig. 15 due to the strong finite-size effects.

In Fig. 16 the x component of the susceptibility for the semifrustrated model is shown. This quantity has converged to its thermodynamic limit, and it exhibits a Curie divergence at low temperatures. The ground-state value is dependent on the next-nearest-neighbor coupling $J(\sqrt{2})$, as is clearly demonstrated by plotting two different ratios $J(\sqrt{2})=J(1)$, and $J(\sqrt{2})=0$ (only nearest-neighbor interactions) in Fig. 16.

VI. CONCLUSION

We have studied a recently introduced meron solution[20] to the sign problem within the SSE method. We investigated the sign problem arising in frustrated spin systems and showed that the meron solution can be applied to a particular semifrustrated model. The problems arising when applying the meron ideas to more general models of frustrated spins were discussed. We found that loop algorithms typically are not ergodic and merons do not exist. The sign problem then persists.

For models where the meron solution works we showed that the sign problem can be completely eliminated for certain variables and largely eliminated for other variables. This total and partial elimination comes from a mapping of positive- to negative-weight contributions and involves no approximation. For the variables where the sign problem is almost eliminated the statistical errors can be reduced using a reweighting technique.[20] We studied how the relative statistical error behaves as a function of lattice size with and without reweighting, and showed that the reweighting does not change the scaling behavior but significantly reduces the overall magnitude of the fluctuations.

It is evident that the meron solution suffers from the same problem in both frustrated spin and fermionic systems—it is confined to a few special cases. It would be of great importance to be able to extend it to more general cases, e.g., by working in basis where the required loop structure appears. The possibility of finding such bases should be explored.

ACKNOWLEDGMENTS

The research was supported by NSF Grants Nos. DMR-9629987 and DMR-9712765. P.H. acknowledges support by Finska Vetenskaps-Societeten and Suomalainen Tiedeakatemia.

*Present address: Department of Theoretical Physics, Royal Institute of Technology, SE-10044 Stockholm, Sweden.

[1] For reviews of quantum Monte Carlo methods and applications, see, e.g, D. Scalapino, in *Frontiers and Border Lines of Many-Particle Physics*, Proceedings International School of Physics ''Enrico Fermi,'' 1987, edited by R.A. Broglia and J.R. Schrieffer (Elsevier Science, Amsterdam, 1988); W. Von Der Linden, Phys. Rep. **220**, 53 (1992); A. W. Sandvik, in *Strongly Correlated Magnetic and Superconducting Systems*, Proceedings of the 1996 El Escorial Summer School, edited by G. Sierra and M. A. Martin Delgado (Springer-Verlag, Berlin, 1997).

[2] M. Suzuki, Prog. Theor. Phys. **56**, 1454 (1976); M. Suzuki, S. Miyashita, and A. Kuroda, **58**, 1377 (1977); M. Barma and B.S. Shastry, Phys. Rev. B **18**, 3351 (1977).

[3] J.E. Hirsch, R.L. Sugar, D.J. Scalapino, and R. Blankenbecler, Phys. Rev. B **26**, 5033 (1982).

[4] R. Blankenbecler, D.J. Scalapino, and R.L. Sugar, Phys. Rev. D **24**, 2278 (1981).

[5] A.W. Sandvik and J. Kurkijärvi, Phys. Rev. B **43**, 5950 (1991); A.W. Sandvik, J. Phys. A **25**, 3667 (1992).

[6] A.W. Sandvik, Phys. Rev. B **56**, 11 678 (1997).

[7] A.W. Sandvik, Phys. Rev. B **59**, R14 157 (1999).

[8] D.C. Handscomb, Proc. Cambridge Philos. Soc. **58**, 594 (1962); **60**, 115 (1964).

[9] J.W. Lyklema, Phys. Rev. Lett. **49**, 88 (1982).

[10] D.H. Lee, J.D. Joannopoulos, and J.W. Negele, Phys. Rev. B **30**, 1599 (1984).

[11] N.V. Prokof'ev, B.V. Svistunov, and I.S. Tupitsyn, Pis'ma Zh. Éksp. Teor. Fiz. **64**, 853 (1996) [JETP Lett. **64**, 911 (1996)]; Zh. Éksp. Teor. Fiz. **114**, 570 (1998) [JETP **87**, 311 (1998)].

[12] B.B. Beard and U.-J. Wiese, Phys. Rev. Lett. **77**, 5130 (1996).

[13] A.W. Sandvik, R.R.P. Singh, and D.K. Campbell, Phys. Rev. B **56**, 14 510 (1997).

[14] S.M.A. Rombouts, K. Heyede, and N. Jachowicz, Phys. Rev. Lett. **82**, 4155 (1999).

[15] H.G. Evertz, G. Lana, and M. Marcu, Phys. Rev. Lett. **70**, 875 (1993).

[16] N. Kawashima, J.E. Gubernatis, and H. Evertz, Phys. Rev. B **50**, 136 (1994).

[17] R.H. Swendsen and J.S. Wang, Phys. Rev. Lett. **58**, 86 (1987).

[18] E.Y. Loh Jr. *et al.*, Phys. Rev. B **41**, 9301 (1990).

[19] S. Miyashita, M. Takasu, and M. Suzuki, in *Quantum Monte Carlo Methods in Equilibrium and Nonequilibrium Systems*, edited by M. Suzuki (Springer-Verlag Berlin, 1987).

[20] S. Chandrasekharan and U.-J. Wiese, Phys. Rev. Lett. **83**, 3116 (1999).

[21] G. Murthy, D. Arovas, and A. Auerbach, Phys. Rev. B **55**, 3104 (1997).

[22] M. Troyer and S. Sachdev, Phys. Rev. Lett. **81**, 5418 (1998).